



Ameliorating parkinsonian motor dysfunction by targeting histamine receptors in entopeduncular nucleus–thalamus circuitry

Jian-Ya Peng^{a,1,2}, Zeng-Xin Qi^{b,c,d,e,1}, Qi Yan^{a,1} , Xiu-Juan Fan^{a,1}, Kang-Li Shen^a, Hui-Wei Huang^a, Jian-Hua Lu^a, Xiao-Qin Wang^a, Xiao-Xia Fang^a, Liming Mao^{f,g} , Jianguang Ni^{e,3} , Liang Chen^{b,c,d,e,3} , and Qian-Xing Zhuang^{a,3}

Edited by Peter Strick, University of Pittsburgh Brain Institute, Pittsburgh, PA; received September 23, 2022; accepted March 7, 2023

In Parkinson's disease (PD), reduced dopamine levels in the basal ganglia have been associated with altered neuronal firing and motor dysfunction. It remains unclear whether the altered firing rate or pattern of basal ganglia neurons leads to parkinsonism-associated motor dysfunction. In the present study, we show that increased histaminergic innervation of the entopeduncular nucleus (EPN) in the mouse model of PD leads to activation of EPN parvalbumin (PV) neurons projecting to the thalamic motor nucleus via hyperpolarization-activated cyclic nucleotide-gated (HCN) channels coupled to postsynaptic H₂R. Simultaneously, this effect is negatively regulated by presynaptic H₃R activation in subthalamic nucleus (STN) glutamatergic neurons projecting to the EPN. Notably, the activation of both types of receptors ameliorates parkinsonism-associated motor dysfunction. Pharmacological activation of H₂R or genetic upregulation of HCN2 in EPN^{PV} neurons, which reduce neuronal burst firing, ameliorates parkinsonism-associated motor dysfunction independent of changes in the neuronal firing rate. In addition, optogenetic inhibition of EPN^{PV} neurons and pharmacological activation or genetic upregulation of H₃R in EPN-projecting STN^{Glu} neurons ameliorate parkinsonism-associated motor dysfunction by reducing the firing rate rather than altering the firing pattern of EPN^{PV} neurons. Thus, although a reduced firing rate and more regular firing pattern of EPN^{PV} neurons correlate with amelioration in parkinsonism-associated motor dysfunction, the firing pattern appears to be more critical in this context. These results also confirm that targeting H₂R and its downstream HCN2 channel in EPN^{PV} neurons and H₃R in EPN-projecting STN^{Glu} neurons may represent potential therapeutic strategies for the clinical treatment of parkinsonism-associated motor dysfunction.

histamine | H₂R | H₃R | entopeduncular nucleus | Parkinson's disease

The entopeduncular nucleus (EPN) in rodents or the globus pallidus internus (GPI) in primates is located caudomedial to the striatum. It is one of the primary output nuclei of the basal ganglia along with the substantia nigra pars reticulata. Accumulating evidence suggests that the EPN plays an essential role in several physiological and pathophysiological processes, including motor dysfunction in Parkinson's disease (PD) (1, 2). PD is a common chronic progressive age-related neurodegenerative movement disorder characterized by the loss of dopaminergic neurons in the substantia nigra pars compacta (SNc) (3, 4). This deficit in dopaminergic neurons causes a profound decrease in the dopamine (DA) levels in the basal ganglia and impairs neuronal activity in neurons of the EPN and subthalamic nucleus (STN), such as an increased number of bursting neurons and more irregular and bursty firing activity (5, 6). This suggests that abnormal neuronal firing activity in EPN neurons induced by the loss of dopaminergic neurons may play a role in parkinsonian motor dysfunction. Acute L-dopamine treatment not only reverses the irregular and bursting pattern but also enhances the low firing rate of EPN neurons in 6-hydroxydopamine (6-OHDA)-lesioned rats (5). The classical cortico-basal ganglia-thalamo-cortical motor control circuit is also affected in PD, implying that the EPN influences locomotion via the thalamic motor nucleus, including the ventral medial/ventral anterior and lateral (VM/VAL) nuclei (7–10).

Previous studies have reported that 89% of rodent EPN neurons are γ -Aminobutyric acid (GABA)ergic (8, 11–13). There are at least four different types of GABAergic neurons in the EPN: Calcium-binding protein parvalbumin (PV)-expressing neurons innervate the VM/VAL and parafascicular thalamic nuclei of the thalamus and the pedunculopontine tegmental nucleus of the brainstem (8, 11), and three other types of neurons expressing somatostatin (Sst) and/or nitric oxide synthase (NOS) innervate the lateral habenula (12, 13). Approximately 29% of EPN^{GABA} neurons are PV-positive neurons, which are mainly concentrated in the caudal/posterior two-thirds of the EPN in the center of the nucleus (EPN^{PV}) (13). Neurons expressing Sst and NOS (EPN^{NOS/Sst}) or only Sst (EPN^{Sst})

Significance

The pathology of PD is associated with dysfunction of multiple neuromodulatory pathways in the basal ganglia, including abnormal histamine levels within the globus pallidus internus (GPI) in postmortem PD patients. However, it remains unclear whether histaminergic innervation in the basal ganglia contributes to the parkinsonism-associated motor symptoms. Here, we report that activation of the postsynaptic H₂R and its coupled HCN2 channel in EPN^{PV} neurons regularizes neuronal firing patterns and ameliorates parkinsonism-associated motor dysfunction, whereas presynaptic H₃R activation in EPN-projecting glutamatergic neurons in the STN ameliorates parkinsonism-associated motor dysfunction by reducing the firing rate of EPN^{PV} neurons. Thus, histamine ameliorates parkinsonian motor symptoms by simultaneously reducing the firing rate and regularizing the firing pattern of EPN^{PV} neurons.

The authors declare no competing interest.

This article is a PNAS Direct Submission.

Copyright © 2023 the Author(s). Published by PNAS. This article is distributed under Creative Commons Attribution-NonCommercial-NoDerivatives License 4.0 (CC BY-NC-ND).

¹J.-Y.P., Z.-X.Q., Q.Y., and X.-J.F. contributed equally to this work.

²Present address: State Key Laboratory of Medical Neurobiology and Ministry of Education Frontiers Center for Brain Science, Institutes of Brain Science, Fudan University, Shanghai 200030, China.

³To whom correspondence may be addressed. Email: jguangni@fudan.edu.cn, hschchenliang@fudan.edu.cn, or qxzhuang@ntu.edu.cn.

This article contains supporting information online at <https://www.pnas.org/lookup/suppl/doi:10.1073/pnas.2216247120/-DCSupplemental>.

Published April 17, 2023.

or only NOS (EPN^{NOS}) represent 6.8%, 38.9%, and 20.1% of EPN^{GABA} neurons, respectively, and they are localized in the rostral/anterior half and the shell region of the EPN (10, 12–14). Here, we specifically focused on EPN^{PV} neurons, which project to the VM/VAL and innervate the premotor cortex to initiate and coordinate movement (11).

Hyperpolarization-activated cyclic nucleotide-gated (HCN) channels are encoded by the HCN1–4 gene family and conduct hyperpolarization-activated current (I_h) (15, 16). HCN channels have a unique expression profile and pronounced effects on neuronal excitability, rhythmic activity, and resting membrane potential (17–19). In the mammalian brain, all four HCN channels are widely expressed in most basal ganglia nuclei, including the EPN. In animal models of PD, HCN channel expression and function are altered in neurons of different basal ganglia nuclei, resulting in altered firing properties (15, 20–22). However, the role of HCN channels in regulating the firing parameters (both the firing rate and pattern) of EPN neurons and parkinsonian motor dysfunction remains undetermined.

It is well established that the central histaminergic system, originating from the tuberomammillary nucleus (TMN) of the hypothalamus, innervates almost all brain regions (23, 24). Previous studies have shown that histamine is involved in the regulation of various functions such as the sleep–wake cycle, energy and endocrine homeostasis, synaptic plasticity, and learning via its receptors (23, 25–27). Recent studies have shown that histamine is involved in motor control by affecting basal ganglia nuclei such as the lateral globus pallidus (LGP), striatum, and STN (28–30). Studies on postmortem PD patients have also shown the involvement of histamine in the pathological process of PD, and a significant increase in the histamine concentration was detected in most basal ganglia nuclei, including the putamen, SNc, and globus pallidus, in the brain samples of PD patients (24, 31, 32). Immunohistochemical and receptor autoradiographic studies have demonstrated moderately dense histaminergic fiber innervation of the EPN in rats and guinea pigs and histamine receptors on GPi neurons in postmortem humans and rhesus monkeys (33–35). However, the function of histamine via its receptors on the different EPN neuron types and the underlying molecular signaling mechanisms remain largely unknown.

Therefore, in the present study, we investigated the effect of histaminergic innervation from the TMN on the firing parameters of EPN^{PV} neurons and parkinsonism-associated motor dysfunction. In 6-OHDA-lesioned mice, histamine levels in the EPN increased compensatorily, and histamine regulated the firing pattern of EPN^{PV} neurons by activating the H₂R and its coupled HCN2 channel, thereby ameliorating the motor dysfunction. Meanwhile, by activating H₃R on EPN-projecting STN^{Glu} neurons, histamine also reduced the firing rate of EPN^{PV} neurons and ameliorated motor dysfunction. Both the reduction in the firing rate and the regularization of the firing pattern of EPN^{PV} neurons contributed to the amelioration of parkinsonism-associated motor dysfunction. However, when both the neuronal firing rate and pattern were altered simultaneously, regularizing the firing pattern of EPN^{PV} neurons had a greater effect on ameliorating parkinsonism-associated motor dysfunction.

Results

A Direct Histaminergic Projection from the TMN to the EPN Excites EPN Neurons by Activating Postsynaptic H₂R, whereas this Effect Is Negatively Regulated by Activating Presynaptic H₃R. To label the histaminergic afferent fibers from the TMN that innervate the EPN, we microinjected a recombinant adeno-associated

virus (AAV) encoding mCherry into the TMN and visualized histaminergic fibers in the EPN by immunohistochemistry (Fig. 1A). In the EPN, we detected double-positive histamine and mCherry anterograde fibers from the TMN adjacent to GABAergic neurons, indicating that the histaminergic neurons in the TMN send their fibers directly to the EPN (Fig. 1B and C), and the area density of histaminergic fibers in the EPN, obtained by dividing the fiber area by the total area of the 20 optical dissectors, was $0.045\% \pm 0.0046\%$.

The effect of histamine or histamine receptor agonists/antagonists on EPN neurons was investigated using whole-cell patch-clamp recordings on sagittal mouse brain slices containing the EPN region (Fig. 1D). In total, we recorded 89 EPN neurons, 80 of which responded to histamine and its receptor agonists, and 20 of which were randomly selected to have a diameter of $15.65 \pm 0.39 \mu\text{m}$, a membrane capacitance of $72.88 \pm 4.02 \text{ pF}$, and a resting membrane potential of $-55 \pm 0.79 \text{ mV}$. These results were consistent with those reported in previous studies (10, 12, 13).

We then determined the postsynaptic effect of histamine on EPN neurons. In the presence of tetrodotoxin (TTX; $0.3 \mu\text{M}$), histamine (1 to $30 \mu\text{M}$) elicited a concentration-dependent inward current in EPN neurons (Fig. 1E, Left). The concentration–response curve shows a half-maximal activation (EC₅₀) of EPN neurons with a histamine concentration of $4.13 \mu\text{M}$ (Fig. 1E, Right). Moreover, we used selective histamine receptor agonists and antagonists to determine which histamine receptors mediate the histamine-induced increase in the autonomous firing rate of EPN neurons. In the presence of TTX, the highly selective H₁R agonist 2-pyridylethylamine (2-PyEA) did not affect the recorded EPN neurons (SI Appendix, Fig. S1A), whereas the highly selective H₂R agonist dimaprit induced an inward current in the neurons in a concentration-dependent manner (SI Appendix, Fig. S1B). In addition, ranitidine (0.3 and $1 \mu\text{M}$), a highly selective H₂R antagonist, blocked the dimaprit-induced inward current in a concentration-dependent manner (SI Appendix, Fig. S1C). Furthermore, the highly selective H₄R agonist VUF8430 did not affect the recorded EPN neurons (SI Appendix, Fig. S1D). These results indicate that histamine elicits a significant excitatory response on EPN neurons via postsynaptic H₂R.

Next, we sought to determine the neuron type involved in the EPN response to histamine. The high number of GABAergic neurons in the EPN (11–13) indicated that we should first determine the H₂R distribution in GABAergic neurons. Double immunostaining for GAD67 and H₂R proteins was performed on EPN-containing mouse brain sections. This revealed codistribution of GAD67 and H₂R in EPN cells ($94.57\% \pm 0.86\%$, $n = 20$ sections) (SI Appendix, Fig. S1E). Moreover, after patch-clamp recording, the cytoplasm of visualized EPN neurons was aspirated into the recording pipette for single-cell qPCR. We confirmed the expression of H₂R but not H₁R and H₄R messenger RNAs (mRNAs) in GAD67-positive EPN neurons (SI Appendix, Fig. S1F). These results indicate that H₂R-expressing GABAergic neurons in the EPN exhibit histamine-induced postsynaptic excitation.

We further detected the presynaptic effect of histamine on EPN neurons. Bath application of histamine increased the firing rate of EPN neurons, and coapplication of histamine and the selective H3R antagonist iodophenopropit (IPP) potentiated the effect of histamine (Fig. 1F and G). Moreover, we found that application of 2,3-dioxo-6-nitro-1,2,3,4-tetrahydrobenzo[f]quinoxaline-7-sulfonamide (NBQX) and D-AP5 abolished miniature excitatory postsynaptic currents (mEPSCs) in EPN neurons. The potent and standard H3R agonist (R)-(-)- α -methylhistamine (RAMH) significantly decreased the frequency but not the amplitude of mEPSCs in EPN neurons, whereas application of IPP abolished this effect (SI Appendix,

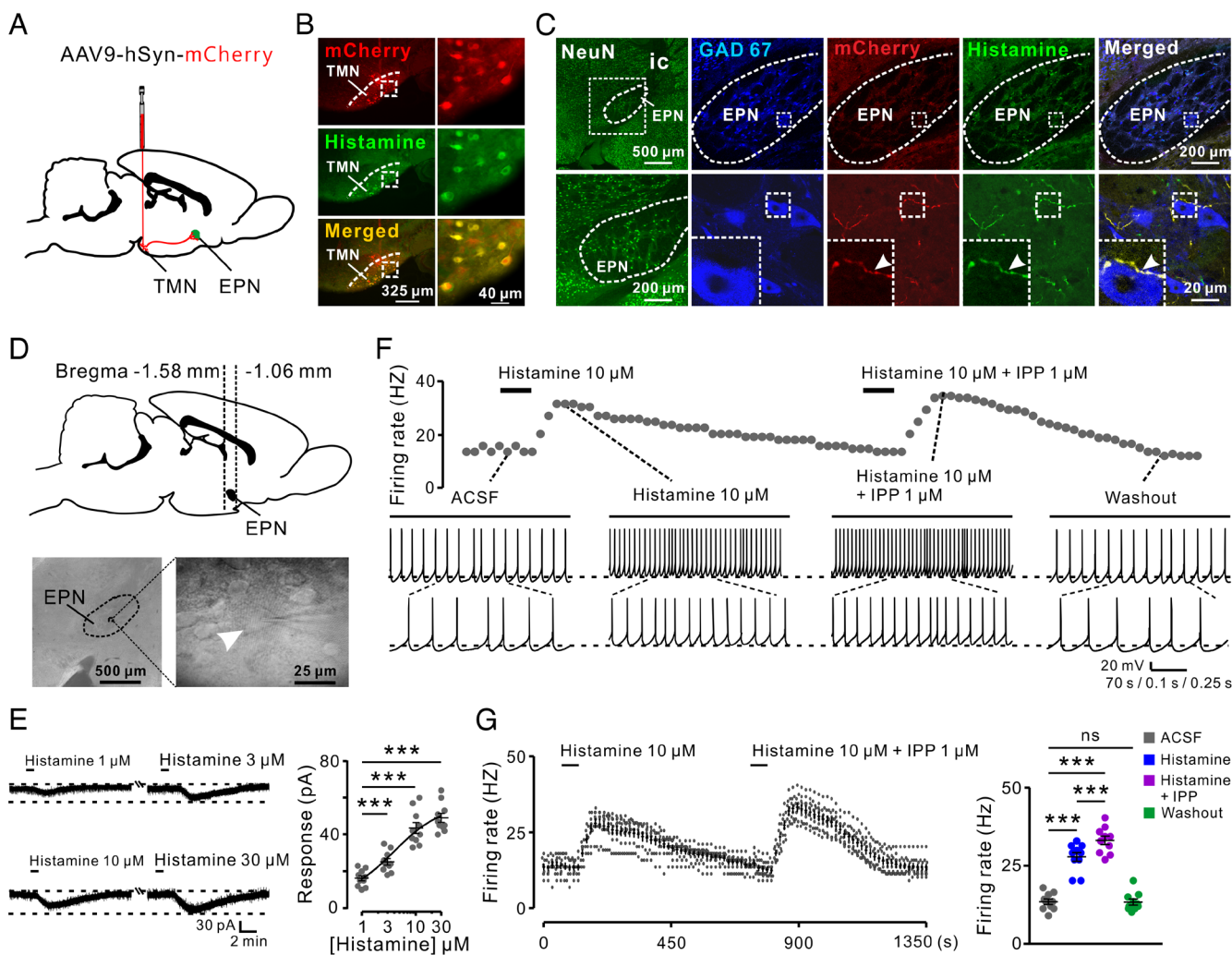


Fig. 1. Histaminergic innervation from the TMN to the EPN excites EPN neurons by activating postsynaptic H₂R, albeit its action is negatively regulated by activating presynaptic H₃R. (A) Diagram depicting the AAV injection and histological reconstruction of the injection map in the TMN region of the mouse brain ($n = 9$). (B) Representative coronal images showing the AAV injection site and histaminergic neurons in the TMN. (C) Left panel: Representative coronal sections with NeuN staining revealed the reference map of the EPN region; Right four panels: Representative coronal images indicate that the histaminergic fibers from the TMN were localized close to the GABAergic EPN neurons (indicated by arrowheads). In these mouse brain sections, the EPN region was immediately below the internal capsule (ic) region. (D) Diagram depicting a sagittal mouse brain section displaying the location of the EPN between -1.06 and -1.58 mm from the bregma and the representative image of coronal brain slices exhibiting the area of the EPN and EPN neurons (indicated by arrowhead) investigated in this mouse. (E) In the voltage-clamp configuration, histamine (1 to 30 μ M) induced an inward current in the recorded EPN neurons in a dose-dependent fashion in the presence of TTX (0.3 μ M), and the concentration–response curves for histamine on the recorded EPN neurons ($n = 10$). (F) In the current clamp configuration, histamine and histamine together with IPP, potent and selective H₂R antagonist, on the firing rate of a recorded EPN neuron and a representative discharge before, during, and after histamine and histamine together with IPP application. (G) The effect of histamine and IPP on the firing rate of the recorded EPN neurons over time and a comparison of the firing rate before histamine application and at the maximum after the application of histamine and histamine together with IPP ($n = 10$). Data are represented as mean \pm SEM; ns, no statistical difference, *** $P < 0.001$.

Fig. S2 A and B. In addition, we found that application of SR95531 prevented miniature inhibitory postsynaptic currents (mIPSCs) in EPN neurons. In contrast, neither RAMH nor IPP affected the amplitude and frequency of mIPSCs in EPN neurons (*SI Appendix*, Fig. S2 C and D), suggesting that presynaptic H₃R activation selectively inhibits glutamatergic but not GABAergic transmission in EPN neurons. Since the EPN receives mainly inhibitory GABAergic afferents from the striatum and LGP and excitatory glutamatergic afferents from the STN, we further determined the distribution of H₃R in EPN-projecting striatum^{GABA}, LGP^{GABA}, and STN^{Glu} neurons. We injected retrograde virus to label GABAergic and glutamatergic neurons projecting to the EPN, respectively (*SI Appendix*, Fig. S2 E and F). We found that H₃R is selectively expressed in EPN-projecting STN^{Glu} but not in striatum^{GABA} and LGP^{GABA} neurons (*SI Appendix*, Fig. S2 G), indicating that activation of H₃R in EPN-projecting STN^{Glu} neurons selectively inhibits glutamatergic transmission in EPN neurons. These results suggest

that histamine excites EPN neurons by activating the postsynaptic H₂R and that this effect is negatively regulated by activation of the presynaptic H₃R.

Histamine-Induced Enhancement of Motor Performance Is Attenuated by Downregulation of H₂R in EPN^{PV} and H₃R in EPN-Projecting STN^{Glu} Neurons. To determine the subtype of GABAergic neurons that mediate the histamine effect in the EPN, we focused on the two largest populations, the EPN^{PV} and EPN^{Sst} neurons (13). We labeled EPN^{PV} and EPN^{Sst} neurons by AAVs in the EPN region of PV-Cre mice (*SI Appendix*, Fig. S3 A) and confirmed that PV neurons are distributed in the posterior region of the EPN, whereas Sst neurons are distributed in the anterior region (*SI Appendix*, Fig. S3 B–F). Therefore, in the following experiments, we injected our viral vectors into the posterior region of the EPN to target EPN^{PV} neurons. To study EPN^{Sst} neurons, we injected the vectors into the anterior region of the EPN.

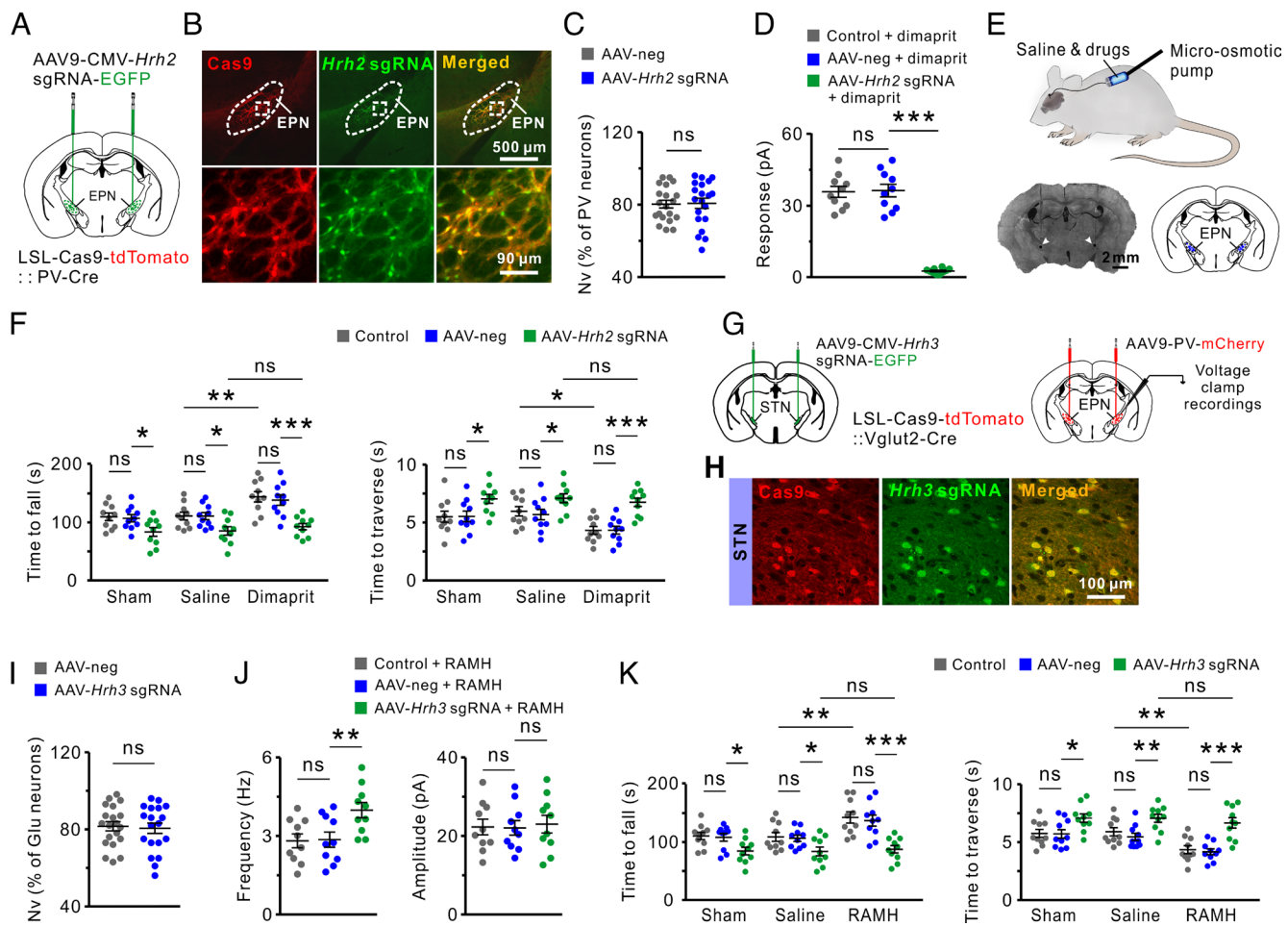


Fig. 2 CRISPR/Cas9-based downregulation of H_2R in EPNPV neurons or H_3R in EPN-projecting STN^{Glut} neurons prevents the histaminergic agonist-induced promotion of motor performance. (A) Schematic of virus injection into the bilateral EPN and histological reconstruction of the injection map in LSL-Cas9-tdTomato::PV-Cre mice ($n = 10$). (B) Representative images depicting Cas9 and *Hrh2* sgRNA expression on EPNPV neurons. (C) Relative quantification in numerical density of EPNPV neurons coexpressed with AAV-neg and AAV-*Hrh2* sgRNA ($n = 20$). (D) Effect of dimaprit (30 μ M) on the inward currents in EPNPV neurons from control, AAV-neg, and AAV-*Hcn2* sgRNA-injected mice ($n = 10$). (E) Schematic diagram of the micro-osmotic pump implanted in the bilateral EPN, the micro-osmotic probe at the injection site (arrowheads) of the EPN, and the histological reconstruction of the injection map of the bilateral EPN across 10 animals after the behavioral test. (F) Bilateral microinfiltration of dimaprit (300 nM) into the EPN in the accelerating rotarod and balance beam tests in control, AAV-neg, and AAV-*Hcn2* sgRNA-injected mice ($n = 10$). (G) Schematic of virus injection into bilateral STN or EPN and histological reconstruction of the injection map in LSL-Cas9-tdTomato::Vglut2-Cre mice ($n = 10$). (H) Representative images displaying Cas9 and *Hrh3* sgRNA expression on STN^{Glut} neurons. (I) Relative quantification in numerical density of STN^{Glut} neurons coexpressed with AAV-neg and AAV-*Hrh3* sgRNA ($n = 20$). (J) The effect of RAMH (10 μ M) on mEPSC frequency and amplitude on EPNPV neurons in control-, AAV-neg-, and AAV-*Hrh3* sgRNA-injected mice ($n = 10$). (K) Bilateral microinfiltration of RAMH (100 nM) into the EPN in the accelerating rotarod and balance beam tests in control-, AAV-neg-, and AAV-*Hrh3* sgRNA-injected mice ($n = 10$). Data are represented as mean \pm SEM; ns, no statistical difference, * $P < 0.05$, ** $P < 0.01$, and *** $P < 0.001$.

We decided to down-regulate H_2R in EPNPV and EPNSSt neurons and H_3R in EPN-projecting STN^{Glut} neurons using CRISPR/Cas9 gene editing. We first down-regulated H_2R in EPNPV neurons by injection of AAV carrying *Hrh2* small guide RNA (sgRNA) into the posterior EPN of double transgenic mice (Fig. 2A), and we found that Cas9 specifically down-regulated H_2R in EPNPV neurons (Fig. 2B). Moreover, we down-regulated H_3R in EPN-projecting STN^{Glut} neurons by injecting AAV carrying *Hrh3* sgRNA into the STN and labeled EPNPV neurons with mCherry of double transgenic mice (Fig. 2G and H). The relative numerical density of neurons infected with AAV neg (control virus) and viruses carrying *Hrh2* sgRNA and *Hrh3* sgRNA confirmed that over 80% of EPNPV and EPN-projecting STN^{Glut} neurons had H_2R and H_3R downregulation, respectively (Fig. 2C and I), and H_2R and H_3R protein levels on EPNPV neurons and EPN-projecting STN^{Glut} neuronal fibers were also significantly reduced after CRISPR-Cas9 activation, respectively (SI Appendix, Fig. S4). Selective downregulation of H_2R in EPNPV neurons and H_3R in EPN-projecting STN^{Glut} neurons blocked dimaprit-induced

inward currents and RAMH-induced reduction of glutamatergic synaptic transmission in EPNPV neurons, further confirming the downregulation efficiency of H_2R and H_3R , respectively (Fig. 2D and J).

We next used a micro-osmotic pump to microinfiltrate histamine receptor agonists into the posterior EPN to assess their effect on motor performance in mice (Fig. 2E), provided that the microdialysis and microinfusion experiments have demonstrated the lack of diffusion of histamine to structures adjacent to the EPN (SI Appendix, Fig. S5). Mice with the specific downregulation of H_2R in EPNPV neurons or H_3R in EPN-projecting STN^{Glut} neurons showed reduced motor performance in the accelerating rotarod (reduced time on the accelerating rotarod) and the balance beam test (increased time to cross the beam) compared to control and AAV-neg-injected mice (Fig. 2F and K). Moreover, either microinfiltration of dimaprit or RAMH promoted motor performance in control and AAV-neg-injected mice, whereas neither microinfiltration of dimaprit nor RAMH had any effect on motor performance in mice with down-regulated H_2R in EPNPV and

H_3R in EPN-projecting STN^{Glu} neurons, respectively (Fig. 2 F and K). Collectively, these results show that histamine promotes motor performance via H_2R in EPN^{PV} and H_3R in EPN-projecting STN^{Glu} neurons.

The EPN^{Sst} neuron-specific downregulation of H_2R was accomplished by bilateral coinjection of AAV carrying *Hrh2* sgRNA and AAV9-Sst-Cre (which delivers Cre recombinase to the EPN^{Sst} neuron) into the anterior EPN of transgenic mice (*SI Appendix*, Fig. S6 A and B). The EPN-projecting STN^{Glu} neuron-specific downregulation of H_3R was accomplished by coinjection of AAV carrying *Hrh3* sgRNA into the STN and AAV9-Sst-mCherry (label EPN^{Sst} neuron) into the anterior EPN of transgenic mice (*SI Appendix*, Fig. S6 F and G). The relative numerical density of neurons infected with AAV-neg, virus carrying *Hrh2* and *Hrh3* sgRNAs confirmed that over 80% of the EPN^{Sst} and EPN-projecting STN^{Glu} neurons had H_2R and H_3R downregulation, respectively (*SI Appendix*, Fig. S6 C and H), and H_2R protein levels on EPN^{Sst} neurons were also significantly reduced after CRISPR-Cas9 activation (*SI Appendix*, Fig. S7). Moreover, selective downregulation of H_2R in EPN^{Sst} neurons and H_3R in EPN-projecting STN^{Glu} neurons blocked dimaprit-induced inward currents and RAMH-induced reduction of glutamatergic synaptic transmission in EPN^{Sst} neurons, thus confirming the efficiency of H_2R and H_3R downregulation, respectively (*SI Appendix*, Fig. S6 D and I). However, mice with specific downregulation of H_2R in EPN^{PV} neurons or H_3R in EPN-projecting STN^{Glu} neurons showed no difference in motor behavior in both tests compared to control and AAV-neg-injected mice regardless of the microinfiltration dimaprit or RAMH into the posterior EPN, respectively (*SI Appendix*, Fig. S6 E and J). All these results indicate that activation of H_2R in EPN^{PV} neurons and H_3R in EPN-projecting STN^{Glu} neurons, but not H_2R in EPN^{Sst} neurons, mediates the effect of histamine on motor performance.

Previous studies have shown that EPN neurons project to the motor thalamus, including the VM/VAL, in rats and mice (8, 9, 11). To assess the projection of the EPN to the VM/VAL, we injected anterograde labeling herpes simplex virus (HSV) expressing enhanced green fluorescent protein (EGFP) and the helper virus into the EPN to confirm the EPN to VM/VAL neuronal connection (*SI Appendix*, Fig. S8A). Subsequent monosynaptic anterograde transmission of HSV from EPN^{PV} neurons to postsynaptic VM/VAL neurons resulted in the EGFP labeling of VM/VAL neurons (*SI Appendix*, Fig. S8B). Moreover, we stereotactically injected cholera toxin subunit B-488 (CTB-488) into the VM/VAL and labeled EPN^{PV} neurons with mCherry (*SI Appendix*, Fig. S8C). We observed that most (83.67% \pm 1.15%, $n = 20$ sections) of the CTB-488-positive neurons were EPN^{PV} neurons (*SI Appendix*, Fig. S8D), which is consistent with the results of previous studies (8–10, 13). The positive results of these retrograde and anterograde tracing experiments indicate that EPN^{PV} neurons project to the VM/VAL.

We also used optogenetics to investigate the contact probability and physiological properties of synaptic connections between EPN^{PV} neurons and VM/VAL neurons. AAV was injected into the posterior EPN to label EPN^{PV} neurons and to express Channelrhodopsin-2 (ChR2) on the neurons (*SI Appendix*, Fig. S8 E and F). An inhibitory postsynaptic current (IPSC) under the voltage clamp (holding potential of 0 mV) was optogenetically evoked in the recorded VM/VAL neurons. We confirmed that this current was monosynaptic because the evoked IPSC was abolished by application of TTX, and this TTX block was reversed by additional application of 4-AP, and we also used SR95531, which completely blocked the evoked IPSC (*SI Appendix*, Fig. S8 G and

H), to demonstrate the GABAergic nature of the evoked events. All these data confirm that GABAergic EPN^{PV} neurons make monosynaptic contacts with VM/VAL neurons.

Studies have shown that a small number of rodent EPN^{PV} neurons also project to the parafascicular thalamic nucleus of the thalamus and the pedunculopontine tegmental nucleus of the brainstem (8, 11, 14). Therefore, we further confirmed the role of H_2R activation in EPN^{PV} neurons in promoting motor performance by downregulating H_2R in neurons retrograde from the VM/VAL to the EPN (*SI Appendix*, Fig. S9A). We found that only H_2R was down-regulated in EPN neurons retrograde from the VM/VAL (*SI Appendix*, Fig. S9B), and downregulation of H_2R in EPN neurons retrograde from the VM/VAL blocked dimaprit-induced inward currents, confirming the downregulation efficiency of H_2R (*SI Appendix*, Fig. S9C). Moreover, mice with the specific downregulation of H_2R in EPN neurons retrograde from the VM/VAL showed reduced motor performance in both tests compared with control and AAV-neg-injected mice (*SI Appendix*, Fig. S9D). This suggests that downregulation of H_2R in EPN neurons retrograde from the VM/VAL prevents the promoting effect of endogenous histamine on motor performance. In addition, microinfiltrating dimaprit into the EPN promoted motor performance in the control and AAV-neg-injected mice but not in mice with the specific downregulation of H_2R in EPN neurons retrograde from the VM/VAL (*SI Appendix*, Fig. S9D), indicating that exogenous histamine promotes motor performance via activation of H_2R in EPN neurons retrograde from the VM/VAL. Taken together, these results demonstrate that in mice, central histaminergic fibers originating from TMN histaminergic neurons can enhance motor performance by directly activating postsynaptic H_2R in EPN^{PV} and presynaptic H_3R in EPN-projecting STN^{Glu} neurons, respectively.

Histamine Levels Are Compensatorily Elevated in the EPN, and Histamine Ameliorates Motor Dysfunction by Activating H_2R and H_3R in 6-OHDA-Lesioned Mice. Previous studies have shown an increase in brain histamine levels in the pathological process of PD (24, 31). Hence, we investigated whether DA reduction leads to increased histamine levels in the mouse brain and whether histamine positively affects motor dysfunction via the TMN-EPN-VM/VAL neuronal signaling pathway described in this study. We confirmed the reduced numerical density of dopaminergic neurons in the ipsilateral SNc of the lesioned side compared to the contralateral untreated side 3 d after 6-OHDA treatment (*SI Appendix*, Fig. S10 A and B). Consistent with dopaminergic cell loss, we also found that histamine levels in microdialysis samples from the EPN region and histaminergic fiber area density in the EPN were significantly increased on the lesioned side compared to the untreated side 3 d after 6-OHDA treatment (Fig. 3 A and B and *SI Appendix*, Fig. S10C).

We bilaterally microinfiltrated the EPN *in vivo* with drugs affecting histamine signaling to analyze the effect of histamine on motor dysfunction in 6-OHDA-lesioned mice (*SI Appendix*, Fig. S10D) and subsequently determined alterations in the adhesive removal test, gait test, and pole test. We found that the microinfiltration of histamine, dimaprit, or RAMH into the posterior EPN ameliorated the motor dysfunction by decreasing the adhesive removal time, prolonging the stride length, and decreasing the time to turn to orient downward and the total time to traverse the rod compared to that in the saline-treated mice (Fig. 3 C–E). Interestingly, infusion of histamine with ranitidine or IPP prevented the amelioration effect of histamine on motor dysfunction (Fig. 3 C–E). These data suggest that in 6-OHDA-lesioned mice, elevated histamine levels in the EPN can be considered a compensatory mechanism that activates

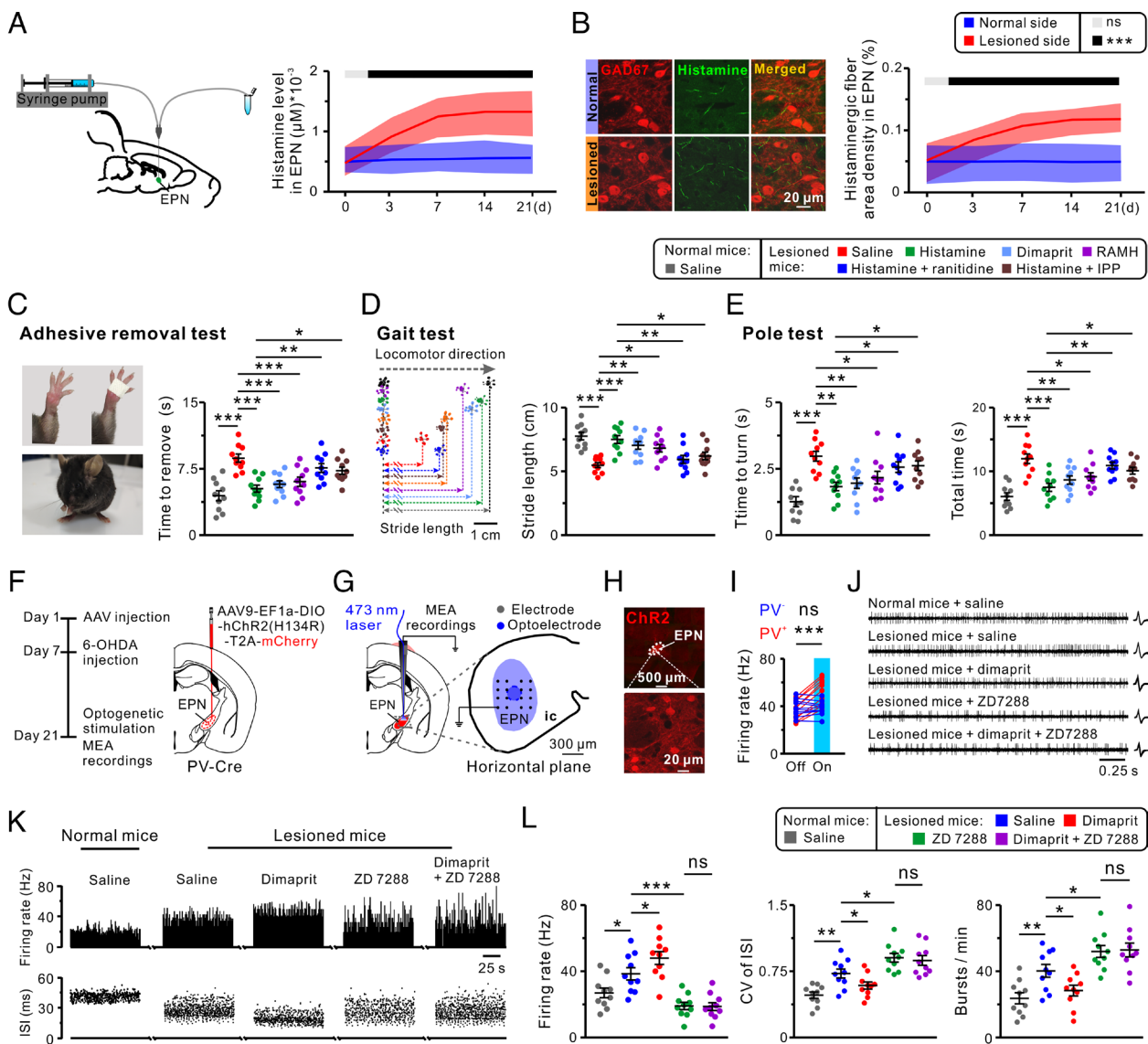


Fig. 3. Histamine levels are compensatorily elevated in the EPN, and histamine ameliorates motor dysfunction by activating H_2R and H_3R , and blocking HCN channels on EPN^{PV} neurons prevents the effect of dimaprit by decreasing the neuronal firing rate and irregularizing the neuronal firing pattern in 6-OHDA-lesioned mice. (A) Histamine levels in the EPN from the same group of 10 mice at the various time points (0, 3, 7, 14, and 21 d) in normal and 6-OHDA-lesioned sides. (B) Area density of histaminergic afferent fibers in the EPN from different groups of 10 mice at each time point (0, 3, 7, 14, and 21 d) in normal and 6-OHDA-lesioned sides. (C–E) Ipsilateral microinfiltration of saline, histamine (100 nM), dimaprit (300 nM), RAMH (100 nM), histamine (100 nM) together with ranitidine (3 nM), and histamine (100 nM) together with IPP (10 nM) into the EPN on motor performance in the adhesive removal test, gait test, and pole test in normal and 6-OHDA-lesioned mice ($n = 10$). (F) Diagram depicting the experimental timeline, virus injection into the EPN, and histological reconstruction of the injection map ($n = 10$ mice). (G) MEA integrated with optogenetic fiber implanted in the EPN of PV-Cre mice. (H) Representative images of the EPN neurons expressing ChR2. (I) ChR2-expressing EPN^{PV} neurons excited by optogenetic stimulation were used for further analysis ($n = 10$). (J) Representative oscilloscope traces, firing rate, and ISI indicate the firing activity of EPN^{PV} neurons when saline, dimaprit (300 nM), ZD7288 (100 nM), and ZD7288 (100 nM) together with dimaprit (300 nM) were microinfiltrated into the EPN using a micro-osmotic pump in normal and 6-OHDA-lesioned free-moving mice. (L) Group data indicating the effect of dimaprit, ZD7288, and ZD7288 together with dimaprit on the firing rate, CV of the ISI, and burst rate of EPN^{PV} neurons in normal and 6-OHDA-lesioned mice ($n = 10$). Data are represented as mean \pm SEM; ns, no statistical difference, * $P < 0.05$, ** $P < 0.01$, and *** $P < 0.001$.

H_2R in EPN^{PV} and H_3R in EPN-projecting STN^{Glu} neurons to ameliorate motor dysfunction.

Pharmacological Blockade of HCN Channels in EPN^{PV} Neurons Reduces Neuronal Firing Rates and Irregular Neuronal Firing Patterns and Prevents the Beneficial Effect of Dimaprit on these Parameters in 6-OHDA-Lesioned Mice. We first determined the ionic mechanism downstream of H_2R . Previous studies have shown that H_2R elicits I_h through the coupled HCN channel (25, 29, 30). To elucidate the ionic mechanisms underlying H_2R -induced excitability of EPN^{PV} neurons, we performed whole-cell patch-clamp recordings on labeled EPN^{PV} neurons *in vitro* (SI Appendix, Fig. S11A). We found that dimaprit mimicked the

histamine-induced inward current, which was almost entirely blocked by ranitidine or ZD7288 (SI Appendix, Fig. S11B), whereas the dimaprit-induced inward current was almost completely antagonized by the adenylate cyclase antagonist SQ 22536 [9-(Tetrahydro-2'-furyl)adenine] and 2',5'-dideoxyadenosine (SI Appendix, Fig. S11 C and D). Moreover, when EPN^{PV} neurons were stepwise exposed to different current amplitudes for 1 s, dimaprit significantly increased and ZD7288 decreased neuronal excitability (SI Appendix, Fig. S11 E and F). These results suggest that HCN channels mediate histamine-induced excitability of EPN^{PV} neurons via the H_2R .

We also found that dimaprit remarkably increased the voltage sag triggered by a hyperpolarizing current pulse and I_h activation

in the current-clamp configuration, whereas ZD7288 prevented the voltage sag both in the absence and presence of dimaprit (*SI Appendix*, Fig. S12A). Moreover, we conducted a series of 1-s hyperpolarizing voltage steps (ranging from -50 to -120 mV in 10 mV steps) to determine the effect of dimaprit on I_h activation (*SI Appendix*, Fig. S12B) and found that dimaprit shifted the I_h activation curve of EPN^{PV} neurons in the direction of the depolarizing voltage and decreased the value of the half-activation potential ($V_{1/2}$) and the activation time constant (τ_{on}) of the neurons compared to the control group (*SI Appendix*, Fig. S12 C–E). In addition, H₂R and HCN1–4 mRNAs are expressed in EPN^{PV} neurons (*SI Appendix*, Fig. S12F). Thus, our results demonstrate that HCN channels are coupled to the H₂R signaling pathway to mediate the excitatory effect of histamine on EPN^{PV} neurons.

Next, we studied the effect of 6-OHDA lesions on HCN channels in mice. We injected AAV to label EPN^{PV} neurons and express ChR2 on the neurons in 6-OHDA-lesioned mice (Fig. 3F). We found that HCN1–4 mRNAs on EPN^{PV} neurons were progressively down-regulated in 6-OHDA-lesioned mice (*SI Appendix*, Fig. S13 A–D), consistent with the results of the previous study (21). Considering HCN channels have distinctive effects on neuronal firing activities (18, 19), we detected firing activities (the firing rate and pattern) of EPN^{PV} neurons using multielectrode array (MEA) recordings *in vivo* (Fig. 3G) or cell-attached recordings *in vitro* in the normal and 6-OHDA-lesioned mice. Only neurons labeled with mCherry *in vitro* (Fig. 3H) or excited by optogenetic stimulation *in vivo* (Fig. 3I) were considered as EPN^{PV} neurons and selected for further recordings. We found that the firing rate and pattern of EPN^{PV} neurons were increased and became irregularized [increased the coefficient of variation (CV) of interspike interval (ISI) and burst rate], respectively, both *in vivo* (*SI Appendix*, Fig. S13E) and *in vitro* (*SI Appendix*, Fig. S13F) in the 6-OHDA-lesioned mice.

We further assessed the role of H₂R activation in the firing rate and pattern of EPN^{PV} neurons in 6-OHDA-lesioned mice. We found that microinfiltration or bath application of dimaprit to the posterior EPN increased the firing rate and regularized the firing pattern (decreased the CV of ISI and burst rate), and ZD7288 decreased the firing rate, irregularized the firing pattern of EPN^{PV} neurons, and also prevented the effect of dimaprit on EPN^{PV} neurons both *in vivo* and *in vitro* (Fig. 3 J–L and *SI Appendix*, Fig. S14 A and B). These results, together with the increased firing rate and irregular firing pattern of EPN^{PV} neurons and the fact that microinfiltration of dimaprit ameliorated parkinsonian motor dysfunction, led us to speculate that the firing pattern of EPN^{PV} neurons may account for the amelioration of motor dysfunction in 6-OHDA-lesioned mice.

Upregulation Rather than Downregulation of HCN2 in EPN^{PV} Neurons Regularizes Neuronal Firing Patterns and Ameliorates Motor Dysfunction in 6-OHDA-Lesioned Mice. Next, we aimed to determine the role of HCN channels in the firing rate and pattern of EPN^{PV} neurons and motor dysfunction in 6-OHDA-lesioned mice. Four HCN channel subtypes have been identified in mammals (17), and all of these subtypes were localized and expressed on EPN^{PV} neurons (*SI Appendix*, Fig. S12F). We first assessed which subtype(s) of HCN channels play(s) a role in motor dysfunction in 6-OHDA-lesioned mice. We performed CRISPR/Cas9 gene editing to selectively down-regulate HCN1–4 and also delivered ChR2 to EPN^{PV} neurons of double transgenic mice (Fig. 4 A and B). EPN^{PV} neurons were identified and recorded using optogenetic stimulation integrated with MEA recordings *in vivo*, and only neurons excited by optogenetic stimulation were considered EPN^{PV} neurons and selected for further recordings

(Fig. 4C). The relative numerical density of neurons infected by AAV neg and virus carrying *Hcn1–4* sgRNAs confirmed that over 80% of EPN^{PV} neurons had the downregulation of HCN1–4, respectively (*SI Appendix*, Fig. S15A); selective downregulation of HCN2 in EPN^{PV} neurons blocked dimaprit-induced inward currents (*SI Appendix*, Fig. S15 B and C), and HCN2 protein levels on EPN^{PV} neurons were also significantly reduced after CRISPR-Cas9 activation (*SI Appendix*, Fig. S15 D–F).

We found that downregulation of HCN2 instead of HCN1, HCN3, and HCN4 in EPN^{PV} neurons decreased the neuronal firing rate, irregularized the neuronal firing pattern, and prevented the effect of dimaprit on the neuronal firing rate and pattern (Fig. 4 D–F). Moreover, downregulation of HCN2 in EPN^{PV} neurons further aggravated motor dysfunction by increasing the adhesive removal time, shortening the stride length, and increasing the time to turn to orient downward and the total time to traverse the rod and also prevented the amelioration of motor dysfunction caused by the microinfiltration of dimaprit (Fig. 4 G–I). In addition, selective downregulation of HCN2 and H₂R in EPN^{PV} neurons reduced neuronal excitability and resting membrane potential (*SI Appendix*, Fig. S15 G–J). All these results suggest that downregulation of the H₂R-coupled HCN2 channel in EPN^{PV} neurons decreases neuronal firing rate, irregularizes neuronal firing pattern, and aggravates motor dysfunction in 6-OHDA-lesioned mice.

We further investigated the role of HCN2 channels in firing activity and motor dysfunction by up-regulating HCN2 in EPN^{PV} neurons of 6-OHDA-lesioned mice. We delivered HCN2 and ChR2 to EPN^{PV} neurons of PV-Cre mice (*SI Appendix*, Fig. S16 A and B); only neurons excited by optogenetic stimulation were considered EPN^{PV} neurons and selected for further recordings (*SI Appendix*, Fig. S16C), and upregulation of HCN2 in EPN^{PV} neurons potentiated dimaprit-induced inward currents, further confirming the upregulation efficiency of HCN2 (*SI Appendix*, Fig. S16D).

In contrast to downregulation, upregulation of HCN2 in EPN^{PV} neurons increased neuronal firing rate, regularized neuronal firing pattern, and also promoted the effect of dimaprit on the neuronal firing rate and pattern (*SI Appendix*, Fig. S16 E–G). In addition, upregulation of HCN2 in EPN^{PV} neurons ameliorated motor dysfunction by decreasing adhesive removal time, prolonging stride length, and decreasing downward orientation and total rod traversal time and also promoted the amelioration of motor dysfunction by dimaprit (*SI Appendix*, Fig. S16 H–J). Taken together, these results suggest that histamine regularized the firing pattern of EPN^{PV} neurons and ameliorated the motor dysfunction in 6-OHDA-lesioned mice by activating the H₂R-coupled HCN2 channel, which was independent of the changes in the neuronal firing rate.

Optogenetic Inhibition Rather than Activation of HCN2-Up-Regulated EPN^{PV} Neurons Further Ameliorates Motor Dysfunction in 6-OHDA-Lesioned Mice. We further investigated the role of the firing rate of EPN^{PV} neurons in motor dysfunction in 6-OHDA-lesioned mice. We delivered ChR2 and eNpHR3.0 into EPN^{PV} neurons, and in some groups, HCN2 was also up-regulated in EPN^{PV} neurons of PV-Cre mice (*SI Appendix*, Fig. S17A). An optoelectrode integrated with multiarray electrode was implanted into the EPN to manipulate EPN^{PV} neurons, and ChR2-expressing EPN^{PV} neurons excited by blue light stimulation and eNpHR3.0-expressing EPN^{PV} neurons inhibited by yellow light stimulation were considered EPN^{PV} neurons and selected for further recordings (*SI Appendix*, Fig. S17B). Optogenetic inhibition of EPN^{PV} neurons decreased the neuronal firing rate but not the pattern and ameliorated motor dysfunction by decreasing adhesive removal time, prolonging stride length, and

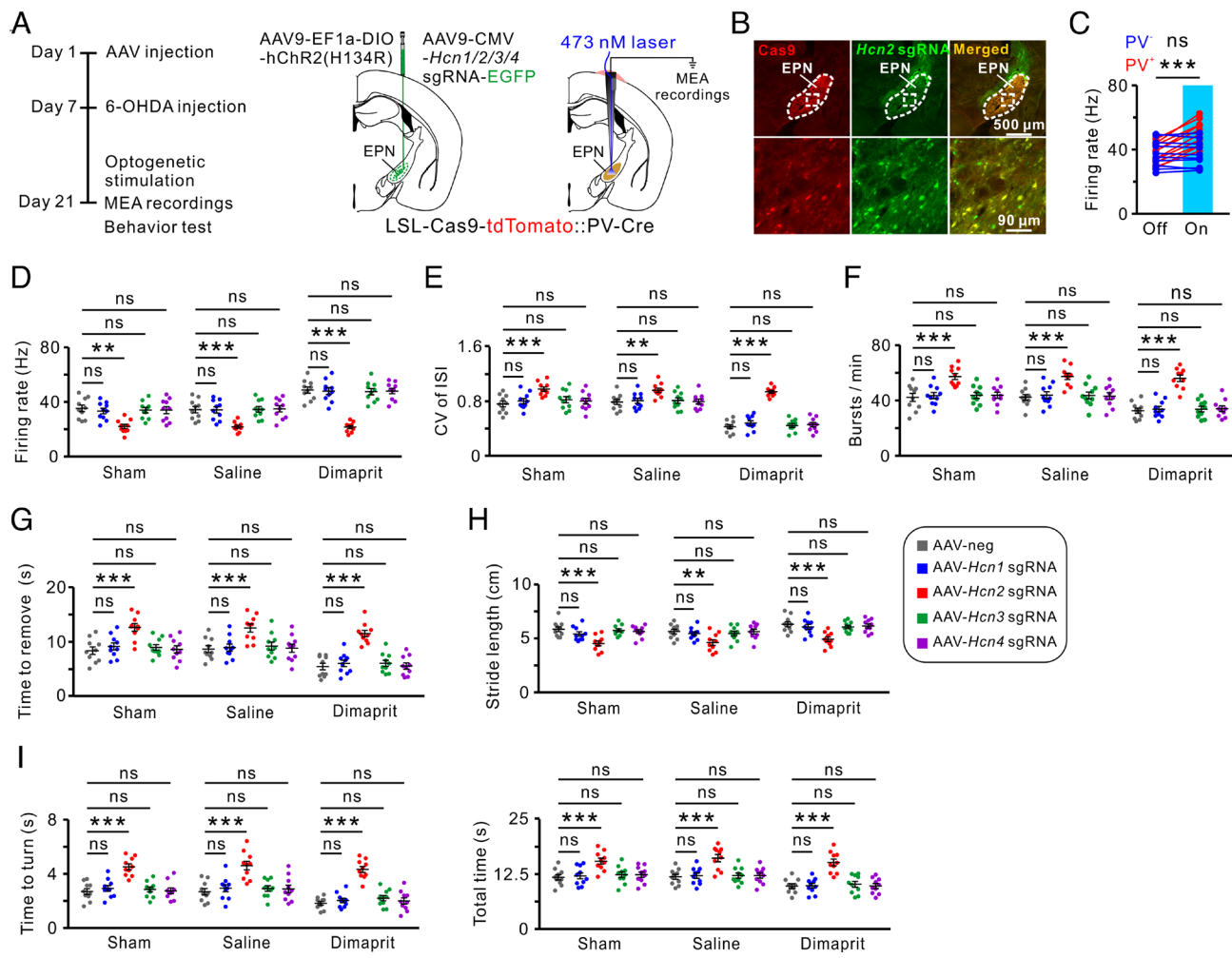


Fig. 4. CRISPR/Cas9-based downregulation of HCN2 in EPN^{PV} neurons aggravates motor dysfunction and prevents the ameliorating effect of dimaprit in 6-OHDA-lesioned mice. (A) Diagram depicting the experimental timeline, virus injection into the EPN, histological reconstruction of the injection map, and optogenetic stimulation-integrated MEA recordings of EPN^{PV} neurons in 6-OHDA-lesioned LSL-Cas9-tdTomato::PV-Cre mice ($n = 20$). (B) Representative image of a coronal brain slice displaying expression of Cas9, sgRNA, and coexpression of Cas9 and sgRNA on the same EPN^{PV} neurons. (C) ChR2-expressing EPN^{PV} neurons excited by optogenetic activation were used for further analysis ($n = 10$). (D–F) CRISPR/Cas9-based downregulation of HCN1–4 on the firing rate, CV of ISI, and burst rate of EPN^{PV} neurons upon microinfiltration of saline or dimaprit into the EPN ($n = 10$). (G–I) Downregulation of HCN1–4 in EPN^{PV} neurons on motor dysfunction in the adhesive removal test, gait test, and pole test during microinfiltration of saline or dimaprit into the EPN ($n = 10$). Data are represented as mean \pm SEM; ns, no statistical difference; ** $P < 0.01$ and *** $P < 0.001$.

decreasing downward orientation time and total rod traversal time. Interestingly, although upregulation of HCN2 in EPN^{PV} neurons ameliorated parkinsonism-associated motor dysfunction, optogenetic inhibition of HCN2-up-regulated EPN^{PV} neurons further ameliorated parkinsonism-associated motor dysfunction by reducing the neuronal firing rate without affecting the pattern, whereas optogenetic activation of EPN^{PV} neurons had the opposite effect (SI Appendix, Fig. S17 C–J), suggesting that the neuronal firing rate is also closely related to parkinsonian motor dysfunction. Moreover, optogenetic activation or inhibition of EPN^{PV} neurons expressing control virus has no effect on the neuronal firing rate and pattern (SI Appendix, Fig. S18). These results suggest that in addition to the firing pattern of EPN^{PV} neurons, a decrease in neuronal firing rate is strongly associated with the amelioration of motor dysfunction in 6-OHDA-lesioned mice.

Upregulation Rather than Downregulation of H₃R in EPN-Projecting STN^{Glu} Neurons Increases the Firing Rate of EPN^{PV} Neurons and Aggravates Motor Dysfunction in 6-OHDA-Lesioned Mice. To investigate the role of H₃R in EPN-projecting STN^{Glu} neurons in the firing rate and pattern of EPN^{PV} neurons

and motor dysfunction in 6-OHDA-lesioned mice, we first performed CRISPR/Cas9 gene editing to selectively downregulate H₃R in EPN-projecting STN^{Glu} neurons and delivered ChR2 into EPN^{PV} neurons of double transgenic mice (Fig. 5 A and B). ChR2-expressing EPN^{PV} neurons excited by blue light stimulation were considered EPN^{PV} neurons and selected for further recordings (Fig. 5 C). Selective downregulation of H₃R in EPN-projecting STN^{Glu} neurons prevented the effect of RAMH on synaptic transmission of EPN^{PV} neurons, further confirming the downregulation efficiency of H₃R (SI Appendix, Fig. S19). Downregulation of H₃R in EPN-projecting STN^{Glu} neurons increased the firing rate, but did not alter the firing pattern of EPN^{PV} neurons, and aggravated motor dysfunction by increasing the adhesive removal time and shortening the stride length, increasing downward orientation time and total rod traversal time; it also prevented the decrease in firing rate and the amelioration of motor dysfunction induced by microinfiltration of RAMH in the posterior EPN of 6-OHDA-lesioned mice (Fig. 5 D–I).

We next up-regulated H₃R in EPN-projecting STN^{Glu} neurons and delivered ChR2 into EPN^{PV} neurons of PV-Cre mice (SI Appendix, Fig. S20A). ChR2-expressing EPN^{PV} neurons

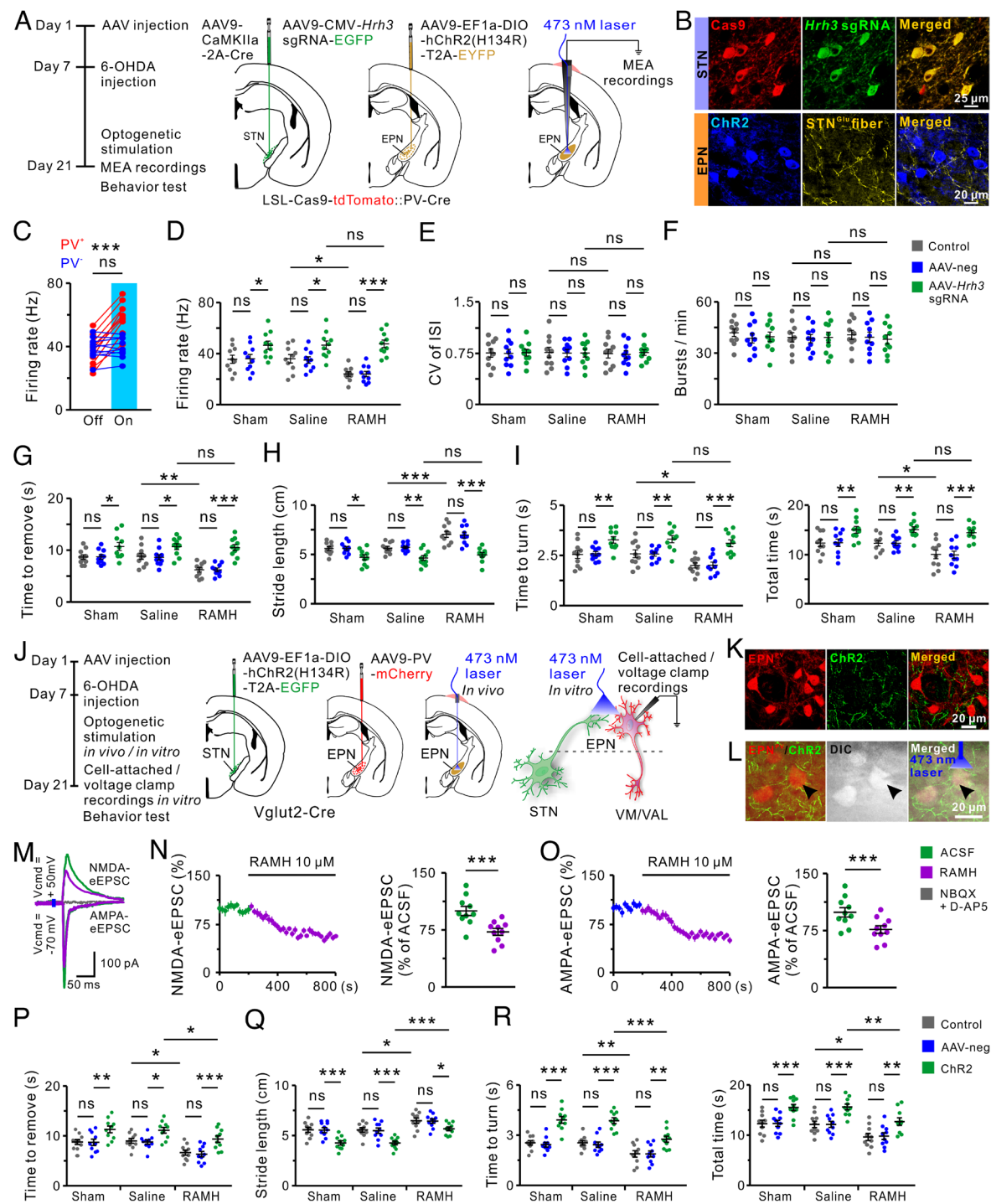


Fig. 5. CRISPR/Cas9-based downregulation of H₃R in EPN-projecting STN^{Glu} neurons increases the firing rate of EPN^{PV} neurons and aggravates the motor dysfunction, whereas pharmacological activation of H₃R on EPN-projecting STN^{Glu} neurons ameliorates motor dysfunction in 6-OHDA-lesioned mice. (A) Diagram depicting the experimental timeline, virus injection into the STN and EPN, histological reconstruction of the injection map, and optogenetic stimulation-integrated MEA recordings of EPN^{PV} neurons in 6-OHDA-lesioned LSL-Cas9-tdTomato::PV-Cre mice ($n = 20$). (B) Upper panel: Representative image of the coronal brain slice displaying Cas9, sgRNA expression, and Cas9 and sgRNA coexpression on the same STN neurons; Lower panel: EPN^{PV} neurons expressing ChR2, and EPN-projecting STN^{Glu} fibers in the EPN. (C) ChR2-expressing EPN^{PV} neurons excited by optogenetic activation were used for further analyses ($n = 10$). (D–F) CRISPR/Cas9-based downregulation of H₃R in EPN-projecting STN^{Glu} neurons on the firing rate, CV of ISI, and burst rate of EPN^{PV} neurons during microinfiltration of saline or RAMH into the EPN ($n = 10$). (G–I) Downregulation of H₃R in EPN-projecting STN^{Glu} neurons on motor dysfunction in the adhesive removal test, gait test, and pole test during microinfiltration of saline or RAMH into the EPN ($n = 10$). (J) Diagram depicting the experimental timeline, virus injection into the STN and EPN, histological reconstruction of the injection map, and optogenetic activation of the axon terminal of EPN-projecting STN^{Glu} neurons in vivo and in vitro in 6-OHDA-lesioned Vglut2-Cre mice ($n = 20$). (K) Representative image displaying EPN^{PV} neurons, and the ChR2-expressing fibers of EPN-projecting STN^{Glu} neurons in the EPN. (L) Representative images displaying EPN^{PV} neurons and EPN-projecting STN^{Glu} fibers under fluorescent field, and EPN^{PV} neurons (arrowhead) under differential interference contrast field were selected for further voltage-clamp recordings. (M) Traces of recorded eEPSCs in EPN^{PV} neurons evoked by the optogenetic activation of glutamatergic afferents were recorded at -70 and +40 mV in ACSF during application of RAMH (3 μM) and coapplication of NBQX (10 μM) and D-AP5 (20 μM). (N and O) Effect of RAMH on the amplitude of AMPA ($N; n = 10$) and NMDA eEPSCs ($O; n = 10$) in EPN^{PV} neurons. (P–R) Microinfiltration of saline or RAMH into the EPN on the motor dysfunction in the adhesive removal test, gait test, and pole test upon optogenetic activation of the EPN-projecting STN^{Glu} terminals in EPN ($n = 10$). Data are represented as mean ± SEM; ns, no statistical difference, * $P < 0.05$, ** $P < 0.01$, and *** $P < 0.001$.

excited by blue light stimulation were considered EPN^{PV} neurons and selected for further recording (*SI Appendix*, Fig. S20*B*). Selective upregulation of H₃R in EPN-projecting STN^{Glu} neurons potentiated the effect of RAMH on synaptic transmission of EPN^{PV} neurons, further confirming the upregulation efficiency of H₃R (*SI Appendix*, Fig. S21). In contrast to H₃R downregulation, upregulation of H₃R in EPN-projecting STN^{Glu} neurons decreased the firing rate of EPN^{PV} neurons, ameliorated motor dysfunction, and also potentiated the effect of RAMH (*SI Appendix*, Fig. S20 *C–H*). All these results suggest that downregulation rather than upregulation of H₃R in EPN-projecting STN^{Glu} neurons decreased the firing rate of EPN^{PV} neurons and aggravated the motor dysfunction of 6-OHDA-lesioned mice.

We further investigated the role of H₃R activation on the EPN^{PV} neuronal firing rate *in vitro*. We delivered ChR2 into EPN-projecting STN^{Glu} neurons and labeled EPN^{PV} neurons with mCherry from Vglut2-Cre mice (Fig. 5 *J* and *K*). We found that RAMH reduced the increase in the firing rate, but not the firing pattern, of EPN^{PV} neurons induced by optogenetic activation of the terminals of EPN-projecting STN^{Glu} neurons *in vitro* (*SI Appendix*, Fig. S22). Moreover, we induced glutamatergic evoked excitatory postsynaptic currents (eEPSCs) in EPN^{PV} neurons by optogenetic activation of EPN-projecting STN^{Glu} terminals (Fig. 5*L*) and found that RAMH consistently suppressed the amplitude of α-amino-3-hydroxy-5-methyl-4-isoxazolepropionic acid (AMPA) and N-methyl-D-aspartate (NMDA) eEPSCs (Fig. 5 *M–O*), suggesting that activation of H₃R in EPN-projecting STN^{Glu} neurons inhibits AMPA- and NMDA-mediated glutamatergic transmission in EPN^{PV} neurons. In addition, optogenetic activation of the terminals of EPN-projecting STN^{Glu} neurons aggravated motor dysfunction by increasing adhesive removal time, shortening the stride length, and increasing downward orientation time and total rod traversal time and also prevented the amelioration of motor dysfunction induced by microinfiltration of RAMH (Fig. 5 *P–R*). Collectively, these results strongly suggest that the firing rate of EPN^{PV} neurons is also closely associated with the amelioration of motor dysfunction and that histamine decreases the firing rate of EPN^{PV} neurons by activating presynaptic H₃R to ameliorate motor dysfunction in 6-OHDA-lesioned mice.

Discussion

A total of four histamine receptors have been identified in the central nervous system, of which H₁R, H₂R, and H₄R are postsynaptic receptors, while H₃R is a presynaptic receptor. The H₂R and its mRNAs are distributed in both guinea pig EPN and monkey GPi (36, 37), and H₃R binding has also been found in both rat EPN and human GPi (38, 39). The H₃R exerts its functions indirectly by regulating the release of many other neurotransmitters, including GABA, glutamate, serotonin, and DA (23, 26, 40). We previously found that intracerebral microinjection of dimaprit promoted motor performance in normal animals and improved motor impairment in animal models of PD (30, 41). In this study, we found that the EPN received projections from the TMN-derived histaminergic fibers. Histamine excited EPN neurons by activating postsynaptic H₂R and negatively regulated this effect by activating H₃R on the EPN-projecting STN^{Glu} neurons. Interestingly, we also found that activation of H₂R and H₃R on EPN^{PV} neurons can both promote motor performance in normal mice and ameliorate motor dysfunction in 6-OHDA-lesioned mice, suggesting that histamine can affect the motor behavior of animals through different mechanisms.

The histamine concentration in many nuclei of basal ganglia increased significantly, and the increased density of histaminergic

fibers and altered morphology of the substantia nigra (SN) were observed in the brains of PD patients (24, 31, 32). We also found that with the degeneration of DA neurons in the SNc, the concentration of histamine and the area density of histaminergic fibers in the EPN gradually increased in 6-OHDA-lesioned mice. These results, together with our current findings, indicate that microinfiltration of histamine into the EPN ameliorates motor dysfunction by activating H₂R and H₃R, which argues that histamine levels in the EPN increase compensatorily during PD pathology and subsequently ameliorate motor dysfunction in 6-OHDA-lesioned mice.

In this study, the concentration of histaminergic drugs used in the patch-clamp recordings of isolated brain slices *in vitro* was approximately 100 times higher than that administered by microinfiltration using a miniosmotic pump *in vivo*. Possible mechanisms include the following: 1) The histaminergic drugs were diluted by the original artificial cerebrospinal fluid (ACSF) in the brain slice bath during the patch-clamp recordings, and 2) when the recorded intact neurons were located deep in the brain slice, the concentration of histaminergic drugs reaching the neuron was lower than that of the perfusate. Therefore, the concentrations of histaminergic drugs that we used in the long-term microinfiltrated release *in vivo* may be close to those that acted on EPN^{PV} neurons. The range of concentrations of histaminergic drugs administered in previous studies has varied widely, which may be due to the differences in the area of the brain affected by histaminergic drugs or in the way they are administered (28, 29, 42).

In autonomous firing neurons in the brain, the HCN channel is considered to be the pacemaker channel of the neuron, which is activated at resting membrane potential and is progressively activated during hyperpolarization. It causes spontaneous depolarization of the pacemaker neuron and triggers action potentials (15, 17). In computational models, downregulation of HCN channel expression leads to burst firing of autonomic firing neurons, suggesting a possible mechanism underlying the emergence of parkinsonism-associated motor dysfunction (28, 43). We found that HCN channels mediate histamine-induced excitability of EPN^{PV} neurons via H₂R, and blocking HCN channels in EPN^{PV} neurons inhibited the effect of dimaprit by decreasing the neuronal firing rate and irregularizing the neuronal firing pattern in 6-OHDA-lesioned mice. Considering the down-regulated expression of HCN channel subtypes in EPN and that altered firing activities of EPN^{PV} neurons are the hallmarks of 6-OHDA-lesioned mice, our results suggest that HCN channel expression in EPN^{PV} neurons is closely associated with the neuronal firing activity and motor dysfunction in PD. These observations are consistent with studies suggesting that HCN channels contribute to parkinsonism-associated motor dysfunction (20, 22), further supporting the potential translational medical value of these channels as therapeutic targets for PD.

Neuronal firing activity, including the firing rate and pattern, encodes and transmits information to distant areas of the brain (44). The EPN is a major output nucleus of the basal ganglia loop, and its projection to the VM/VAL plays an essential role in controlling motor behavior (9, 10). Our results showed that in 6-OHDA-lesioned animal models, upregulation of HCN2 in EPN^{PV} neurons increased the neuronal firing rate, irregularized neuronal firing pattern, and ameliorated motor dysfunction. Alterations in the firing rate and pattern of EPN^{PV} neurons are consistent with the expression of neuronal HCN channels and the physiological functions of HCN channels (19). Nevertheless, single-cell and intraoperative GPi recordings have shown that therapeutic agents, such as levodopa or DA agonists, can significantly reduce GPi firing rates in parkinsonism-associated monkeys and patients, respectively (45). Consistent with this finding, we found that optogenetic inhibition of EPN^{PV} neurons ameliorated

motor dysfunction in 6-OHDA-lesioned mice, while optogenetic inhibition of EPN^{PV} neurons up-regulated HCN2 further ameliorated the motor dysfunction in 6-OHDA-lesioned mice, indicating that a decrease in the firing rate of EPN^{PV} neurons also ameliorated parkinsonian motor dysfunction. Therefore, by regularizing the firing patterns of EPN^{PV} neurons, histamine ameliorates parkinsonian motor dysfunction by activating H₂R and its downstream HCN2 channels. Although activation of HCN2 channels on EPN^{PV} neurons simultaneously triggers changes in the neuronal firing rate and pattern, neuronal firing patterns appear to be more critical in this context.

Although the exact role of H₃R in PD remains unclear, studies have reported that within the basal ganglia, histamine affects glutamate, GABA, and dopaminergic synaptic transmission via presynaptic H₃R (40). In addition, histamine inhibits striatal DA and glutamate release in mice by activating H₃Rs located in dopaminergic and glutamatergic nerve terminals in the nigrostriatal and thalamostriatal pathways, respectively (42, 46). Consistent with this finding, we found that genetic upregulation or pharmacological activation of H₃R in EPN-projecting STN^{Glu} neurons decreased the firing rate of EPN^{PV} neurons without altering the neuronal firing pattern and ameliorated motor dysfunction in 6-OHDA-lesioned mice. Indeed, PD is caused by the degeneration of SN dopaminergic neurons that project to the striatum, resulting in increased activity of indirect pathways in the basal ganglia circuit (6, 47). The glutamatergic projection from the STN to the EPN constitutes an important part of the indirect pathway, and activation of H₃R in EPN-projecting STN^{Glu} neurons ameliorates parkinsonism-associated motor dysfunction by inhibiting indirect pathway activity (40, 48).

To conclude, the present study provides an in-depth analysis of the firing activities of EPN^{PV} neurons in parkinsonism-associated motor dysfunction, including the firing rate and pattern (*SI Appendix*, Fig. S23 and Table S1). Our results revealed that histamine levels in the EPN are compensatorily increased, which subsequently ameliorates parkinsonian motor dysfunction by affecting a population of EPN^{PV} neurons that selectively make monosynaptic contacts with VM/VAL neurons via postsynaptic H₂R and presynaptic H₃R on EPN-projecting STN^{Glu} neurons, respectively. Pharmacological activation (rather than inhibition) HCN2 channel or genetic upregulation (rather than downregulation) of HCN2 in EPN^{PV} neurons regularized neuronal firing patterns independent of the firing rate and ameliorated parkinsonism-associated motor dysfunction. Optogenetic inhibition (rather than activation) of EPN^{PV} neurons and pharmacological activation (rather than inhibition) or genetic upregulation (rather than downregulation) of

H₃R in EPN-projecting STN^{Glu} neurons reduced EPN^{PV} neuron firing rate without altering the firing pattern and ameliorated parkinsonism-associated motor dysfunction. These results demonstrate that although alterations in both firing parameters, firing rate and pattern, of EPN^{PV} neurons correlate with changes in parkinsonian motor dysfunction, the regularized firing pattern of EPN^{PV} neurons is more critical in ameliorating parkinsonism-associated motor dysfunction when both the neuronal firing rate and pattern change simultaneously.

Materials and Methods

Animal care and experiments were conducted in accordance with the U.S. National Institutes of Health Guide for the Care and Use of Laboratory Animals (NIH Publication 85-23, revised 2011) and approved by the Institutional Animal Care and Use Committee of the Nantong University. All efforts were made to minimize the number of animals used and their suffering. The detailed methods for the stereotactic surgery, drug and virus injection, immunohistochemistry and imaging, patch-clamp recording and optogenetic stimulation in vitro, single-cell qPCR, in vivo microdialysis sampling and assay for histamine, combined MEA recordings and optogenetic stimulation on free-moving mice in vivo, behavioral testing, histological identification, and statistical analysis are given in *SI Appendix*.

Data, Materials, and Software Availability. All study data are included in the article and/or *SI Appendix*.

ACKNOWLEDGMENTS. We thank Prof. E. Kramer and Dr. J. Conway (Peninsula Medical School, Faculty of Health University of Plymouth, UK) and Dr. R. Webler (University of Minnesota, USA) for critical comments and suggestions on the manuscript. This work was supported by the National Natural Science Foundation of China (grants 31771143, 81702461, and 32070919); Shanghai Municipal Science and Technology Major Project (No. 2018SHZDZX01), ZJ Lab, and Shanghai Center for Brain Science and Brain-Inspired Technology; Shanghai Sailing Program (17YF1426600); and Postgraduate Research & Practice Innovation Program of Jiangsu Province (KYCX20_2820 and KYCX21_3077).

Author affiliations: ^aDepartment of Physiology, School of Medicine, Nantong University, Nantong, Jiangsu 226001, China; ^bDepartment of Neurosurgery, Huashan Hospital, Shanghai Medical College, Fudan University, Shanghai 200030, China; ^cNational Center for Neurological Disorders, Shanghai 200030, China; ^dShanghai Key Laboratory of Brain Function Restoration and Neural Regeneration, Shanghai 200030, China; ^eState Key Laboratory of Medical Neurobiology and Ministry of Education Frontiers Center for Brain Science, Institutes of Brain Science, Fudan University, Shanghai 200030, China; ^fDepartment of Immunology, School of Medicine, Nantong University, Nantong, Jiangsu 226001, China; and ^gBasic Medical Research Center, School of Medicine, Nantong University, Nantong 226019, China

Author contributions: Q.-X.Z. designed research; J.-Y.P., Z.-X.Q., Q.Y., X.-J.F., K.-L.S., H.-W.H., J.-H.L., X.-Q.W., X.-X.F., and Q.-X.Z. performed research; L.M., J.N., L.C., and Q.-X.Z. analyzed data; and J.N., L.C., and Q.-X.Z. wrote the paper.

1. K. B. Baker *et al.*, Somatotopic organization in the internal segment of the globus pallidus in Parkinson's disease. *Exp. Neurol.* **222**, 219–225 (2010).
2. Y. Mullie, I. Arto, N. Yahiaoui, T. Drew, Contribution of the entopeduncular nucleus and the globus pallidus to the control of locomotion and visually guided gait modifications in the cat. *Cereb. Cortex* **30**, 5121–5146 (2020).
3. M. Fougere *et al.*, Optogenetic stimulation of glutamatergic neurons in the cuneiform nucleus controls locomotion in a mouse model of Parkinson's disease. *Proc. Natl. Acad. Sci. U.S.A.* **118**, e2110934118 (2021).
4. E. M. Adam, E. N. Brown, N. Kopell, M. M. McCarthy, Deep brain stimulation in the subthalamic nucleus for Parkinson's disease can restore dynamics of striatal networks. *Proc. Natl. Acad. Sci. U.S.A.* **119**, e2120808119 (2022).
5. A. Aristieta, J. A. Ruiz-Ortega, T. Morera-Herreras, C. Miguelez, L. Ugedo, Acute L-DOPA administration reverses changes in firing pattern and low frequency oscillatory activity in the entopeduncular nucleus from long term L-DOPA treated 6-OHDA-lesioned rats. *Exp. Neurol.* **322**, 113036 (2019).
6. E. L. McIver *et al.*, Maladaptive downregulation of autonomous subthalamic nucleus activity following the loss of midbrain dopamine neurons. *Cell Rep.* **28**, 992–1002.e1004 (2019).
7. E. G. Jones, *The Thalamus* (Cambridge University Press, Cambridge, ed. 2nd, 2007).
8. E. Kuramoto *et al.*, Two types of thalamocortical projections from the motor thalamic nuclei of the rat: A single neuron-tracing study using viral vectors. *Cereb. Cortex* **19**, 2065–2077 (2009).
9. E. Kuramoto *et al.*, Complementary distribution of glutamatergic cerebellar and GABAergic basal ganglia afferents to the rat motor thalamic nuclei. *Eur. J. Neurosci.* **33**, 95–109 (2011).
10. M. L. Wallace *et al.*, Genetically distinct parallel pathways in the entopeduncular nucleus for limbic and sensorimotor output of the basal ganglia. *Neuron* **94**, 138–152.e135 (2017).
11. H. T. Kha, D. I. Finkelstein, D. V. Pow, A. J. Lawrence, M. K. Horne, Study of projections from the entopeduncular nucleus to the thalamus of the rat. *J. Comp. Neurol.* **426**, 366–377 (2000).
12. Y. Miyamoto, T. Fukuda, Immunohistochemical study on the neuronal diversity and three-dimensional organization of the mouse entopeduncular nucleus. *Neurosci. Res.* **94**, 37–49 (2015).
13. Y. Miyamoto, T. Fukuda, The habenula-targeting neurons in the mouse entopeduncular nucleus contain not only somatostatin-positive neurons but also nitric oxide synthase-positive neurons. *Brain Struct. Funct.* **226**, 1497–1510 (2021).
14. M. Parent, M. Levesque, A. Parent, Two types of projection neurons in the internal pallidum of primates: Single-axon tracing and three-dimensional reconstruction. *J. Comp. Neurol.* **439**, 162–175 (2001).
15. X. Chang, J. Wang, H. Jiang, L. Shi, J. Xie, Hyperpolarization-activated cyclic nucleotide-gated channels: An emerging role in neurodegenerative diseases. *Front. Mol. Neurosci.* **12**, 141 (2019).
16. A. Saponaro *et al.*, A synthetic peptide that prevents cAMP regulation in mammalian hyperpolarization-activated cyclic nucleotide-gated (HCN) channels. *eLife* **7**, e35753 (2018).
17. M. Biel, C. Wahl-Schott, S. Michalakis, X. Zong, Hyperpolarization-activated cation channels: From genes to function. *Physiol. Rev.* **89**, 847–885 (2009).

18. O. Postea, M. Biel, Exploring HCN channels as novel drug targets. *Nat. Rev. Drug Discovery* **10**, 903–914 (2011).
19. B. Santoro, M. M. Shah, Hyperpolarization-activated cyclic nucleotide-gated channels as drug targets for neurological disorders. *Annu. Rev. Pharmacol. Toxicol.* **60**, 109–131 (2020).
20. C. H. Good *et al.*, Impaired nigrostriatal function precedes behavioral deficits in a genetic mitochondrial model of Parkinson's disease. *FASEB J.* **25**, 1333–1344 (2011).
21. C. S. Chan *et al.*, HCN channelopathy in external globus pallidus neurons in models of Parkinson's disease. *Nat. Neurosci.* **14**, 85–92 (2011).
22. J. C. DiFrancesco, D. DiFrancesco, Dysfunctional HCN ion channels in neurological diseases. *Front. Cell. Neurosci.* **6**, 174 (2015).
23. H. L. Haas, O. A. Sergeeva, O. Selbach, Histamine in the nervous system. *Physiol. Rev.* **88**, 1183–1241 (2008).
24. P. Panula, S. Nuutilinen, The histaminergic network in the brain: Basic organization and role in disease. *Nat. Rev. Neurosci.* **14**, 472–487 (2013).
25. R. E. Brown, D. R. Stevens, H. L. Haas, The physiology of brain histamine. *Prog. Neurobiol.* **63**, 637–672 (2001).
26. P. Panula, Histamine receptors, agonists, and antagonists in health and disease. *Handb. Clin. Neurol.* **180**, 377–387 (2021).
27. P. Panula *et al.*, International Union of Basic and Clinical Pharmacology, XCVIII. Histamine Receptors. *Pharmacol. Rev.* **67**, 601–655 (2015).
28. Q. X. Zhuang *et al.*, Regularizing firing patterns of rat subthalamic neurons ameliorates parkinsonian motor deficits. *J. Clin. Invest.* **128**, 5413–5427 (2018).
29. J. Y. Peng *et al.*, Receptor and ionic mechanism of histamine on mouse dorsolateral striatal neurons. *Mol. Neurobiol.* **60**, 183–202 (2023).
30. Z. X. Qi *et al.*, Histamine bidirectionally regulates the intrinsic excitability of parvalbumin-positive neurons in the lateral globus pallidus and promotes motor behaviour. *Br. J. Pharmacol.* 1–29 (2022), 10.1111/bph.16010.
31. J. O. Rinne *et al.*, Increased brain histamine levels in Parkinson's disease but not in multiple system atrophy. *J. Neurochem.* **81**, 954–960 (2002).
32. O. V. Anichtchik, J. O. Rinne, H. Kalimo, P. Panula, An altered histaminergic innervation of the substantia nigra in Parkinson's disease. *Exp. Neurol.* **163**, 20–30 (2000).
33. M. I. Martinez-Mir *et al.*, Three histamine receptors (H1, H2 and H3) visualized in the brain of human and non-human primates. *Brain Res.* **526**, 322–327 (1990).
34. P. Panula, U. Pirvola, S. Auvinen, M. S. Airaksinen, Histamine-immunoreactive nerve fibers in the rat brain. *Neuroscience* **28**, 585–610 (1989).
35. M. S. Airaksinen, P. Panula, The histaminergic system in the guinea pig central nervous system: An immunocytochemical mapping study using an antiserum against histamine. *J. Comp. Neurol.* **273**, 163–186 (1988).
36. M. L. Vizuete *et al.*, Detailed mapping of the histamine H2 receptor and its gene transcripts in guinea-pig brain. *Neuroscience* **80**, 321–343 (1997).
37. M. A. Honrubia, M. T. Vilaro, J. M. Palacios, G. Mengod, Distribution of the histamine H(2) receptor in monkey brain and its mRNA localization in monkey and human brain. *Synapse* **38**, 343–354 (2000).
38. C. Pillot *et al.*, A detailed mapping of the histamine H(3) receptor and its gene transcripts in rat brain. *Neuroscience* **114**, 173–193 (2002).
39. O. V. Anichtchik, N. Peitsaro, J. O. Rinne, H. Kalimo, P. Panula, Distribution and modulation of histamine H(3) receptors in basal ganglia and frontal cortex of healthy controls and patients with Parkinson's disease. *Neurobiol. Dis.* **8**, 707–716 (2001).
40. W. Hu, Z. Chen, The roles of histamine and its receptor ligands in central nervous system disorders: An update. *Pharmacol. Ther.* **175**, 116–132 (2017).
41. Q. X. Zhuang *et al.*, Histamine excites striatal dopamine D1 and D2 receptor-expressing neurons via postsynaptic H1 and H2 receptors. *Mol. Neurobiol.* **55**, 8059–8070 (2018).
42. T. J. Ellender, I. Huerta-Ocampo, K. Deisseroth, M. Capogna, J. P. Bolam, Differential modulation of excitatory and inhibitory striatal synaptic transmission by histamine. *J. Neurosci.* **31**, 15340–15351 (2011).
43. R. Merrison-Hort, R. Borisuk, The emergence of two anti-phase oscillatory neural populations in a computational model of the parkinsonian globus pallidus. *Front. Comput. Neurosci.* **7**, 173 (2013).
44. H. Cagnan *et al.*, Temporal evolution of beta bursts in the parkinsonian cortical and basal ganglia network. *Proc. Natl. Acad. Sci. U.S.A.* **116**, 16095–16104 (2019).
45. S. M. Papa, R. Desimone, M. Fiorani, E. H. Oldfield, Internal globus pallidus discharge is nearly suppressed during levodopa-induced dyskinesias. *Ann. Neurol.* **46**, 732–738 (1999).
46. E. Schlicker, K. Fink, M. Detzner, M. Gotheit, Histamine inhibits dopamine release in the mouse striatum via presynaptic H3 receptors. *J. Neural. Transm. Gen. Sect.* **93**, 1–10 (1993).
47. A. V. Kravitz *et al.*, Regulation of parkinsonian motor behaviours by optogenetic control of basal ganglia circuitry. *Nature* **466**, 622–626 (2010).
48. A. Osorio-Espinoza *et al.*, Pre-synaptic histamine H(3) receptors modulate glutamatergic transmission in rat globus pallidus. *Neuroscience* **176**, 20–31 (2011).